Chemistry & Biology, Volume *20*

Supplemental Information

Knowledge-Based Design of a Biosensor to Quantify Localized ERK Activation in Living Cells

Lutz Kummer, Chia-Wen Hsu, Onur Dagliyan, Christopher MacNevin, Melanie Kaufholz, Bastian Zimmermann, Nikolay V. Dokholyan, Klaus M. Hahn, and Andreas Plückthun

Inventory of Supplemental Information

Supplemental Figure 9 | Control study: Absence of DARPin enrichment in the nucleolus shown by mutation, Related to Figure 4

Supplemental Figure 10 | Control study: direct attachment of DARPin and mCerulean, Related to Figure 4

Supplemental Figure Legends

Supplemental Table 1 | Overview of oligonucleotides

Supplemental Table 1| Overview of oligonucleotides.

oligonucleotide	oligonucleotide sequence (5' → 3')
pE59G91Cf	CTATTCGTTGTCACCTGGAAATTGTTGAAGTTCTGCTG
pE59G91Cr	CAGGTGACAACGAATAGCAGCCAGGTGCAG
pE59G113Cf	CAAATTCTGTAAGACCGCTTTCGACATCTCCATCGAC
pE59G113Cr	GGTCTTACAGAATTTGTCCTGAGCGTTAACGTCAGCAC
pE59N123Cf	CATCGACTGCGGTAACGAGGACCTGGCTGAAATCCTG
pE59N123Cr	GTTACCGCAGTCGATGGAGATGTCGAAAGCGGTCTTAC
pE59G124Cf	GACAACTGTAACGAGGACCTGGCTGAAATCCTG
pE59G124Cr	CTCGTTACAGTTGTCGATGGAGATGTCGAAAGC
pE59D46Af	CGTTAACGCTCTTGACGAGGCGGGTCTTACTC
pE59D46Ar	CAGGTGCAGCGGAGTAAGACCCGCCTCGTC
pE59R90Af	CTGCTATTGCGGGTCACCTGGAAATTGTTGAAGTTC
pE59R90Ar	CAGGTGACCCGCAATAGCAGCCAGGTGCAG
pDST67Cf	AATTCATTAAAGAGGAGAAATTAACTATGAGAGGATCGCATCACCATCACCATCACG
pDST67Cr	GATCCGTGATGGTGATGGTGATGCGATCTTCTCATAGTTAATTTCTCCTCTTTAATG

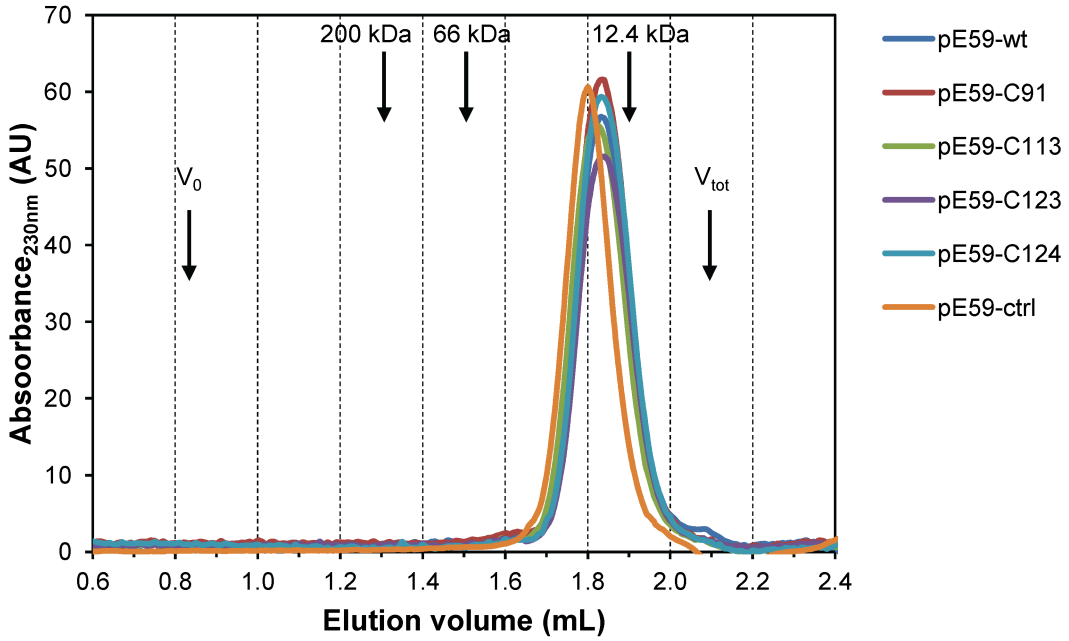

Supplemental Figure 1 | Analytical gel filtration. DARPins were analyzed in PBS supplemented with 1 mM DTT using a Superdex 200 column. The arrows indicate the elution volumes of the marker proteins beta-amylase (200 kDa), BSA (66 kDa) and cytochrome c (12.4 kDa) as well as void (V_0) and total volume (V_{tot}) of the column. Elution profiles of DARPin pE59 (pE59-wt) and pE59 mutants were nearly identical.

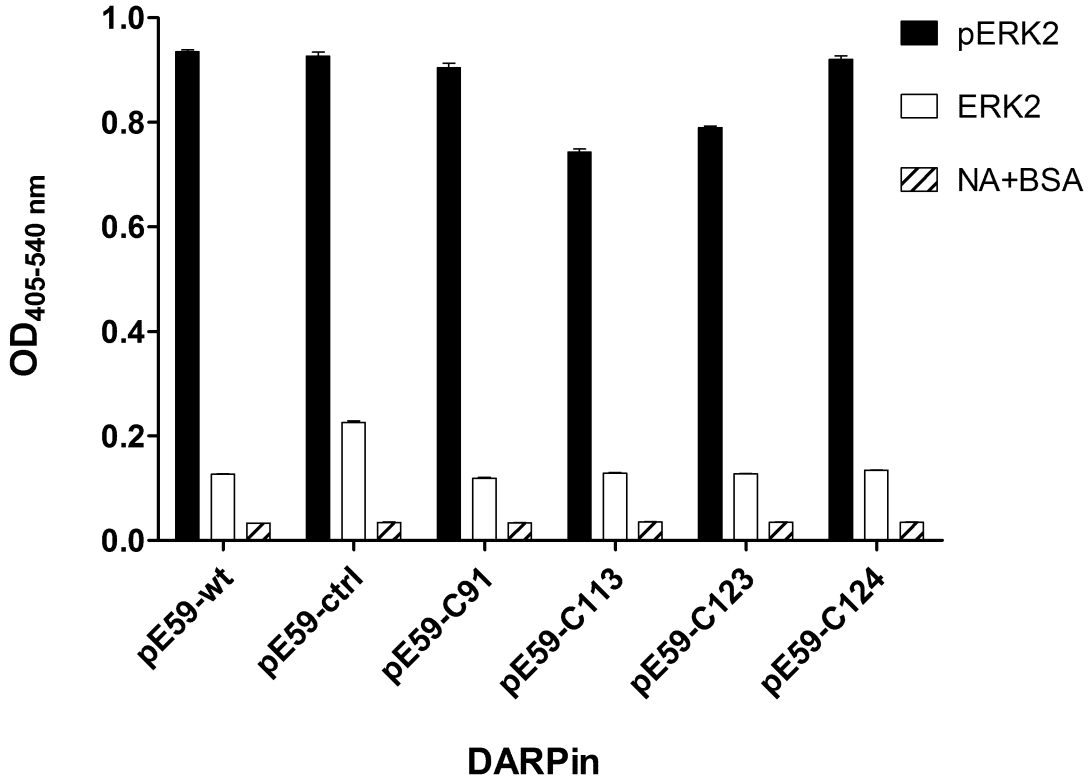

Supplemental Figure 2 | Binding specificity of DARPin pE59 mutants measured by ELISA. DARPin mutants derived from pE59 (pE59-wt) containing a cysteine at designated residues were tested for phosphorylation-specific interaction with ERK2. pE59-ctrl contains a cysteine at the N-terminus of the DARPin, a region which is not implicated in binding to phosphorylated ERK2 (pERK2) as observed in the crystal structure of the complex (Kummer, et al., 2012). In addition, binding to wells with neutravidin (NA) and bovine serum albumin (BSA) was assessed. The absorption was measured at 405 nm with background wavelength correction at 540 nm ($OD_{405\text{-}504\ nm}$).

Mero 53

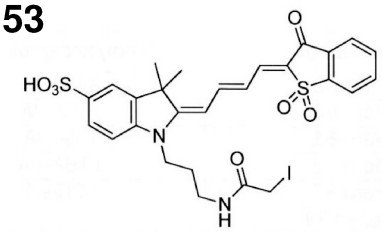

Mero 62

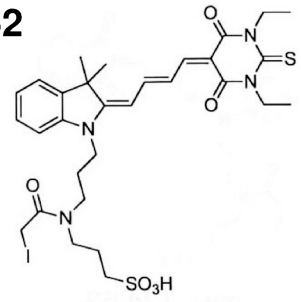

Mero 60

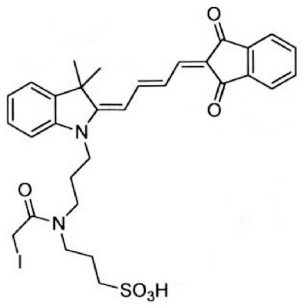

Mero 87

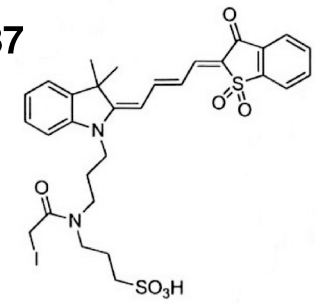

Mero 61

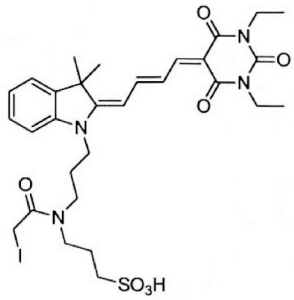

Mero 199

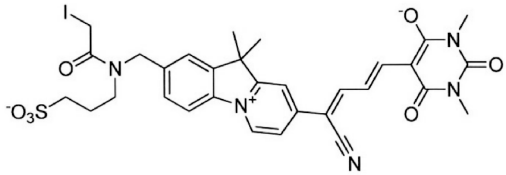

Supplemental Figure 3 | Merocyanine dyes. Structures of the environmentally sensitive merocanine dyes tested on the pERK2-binding DARPin pE59.

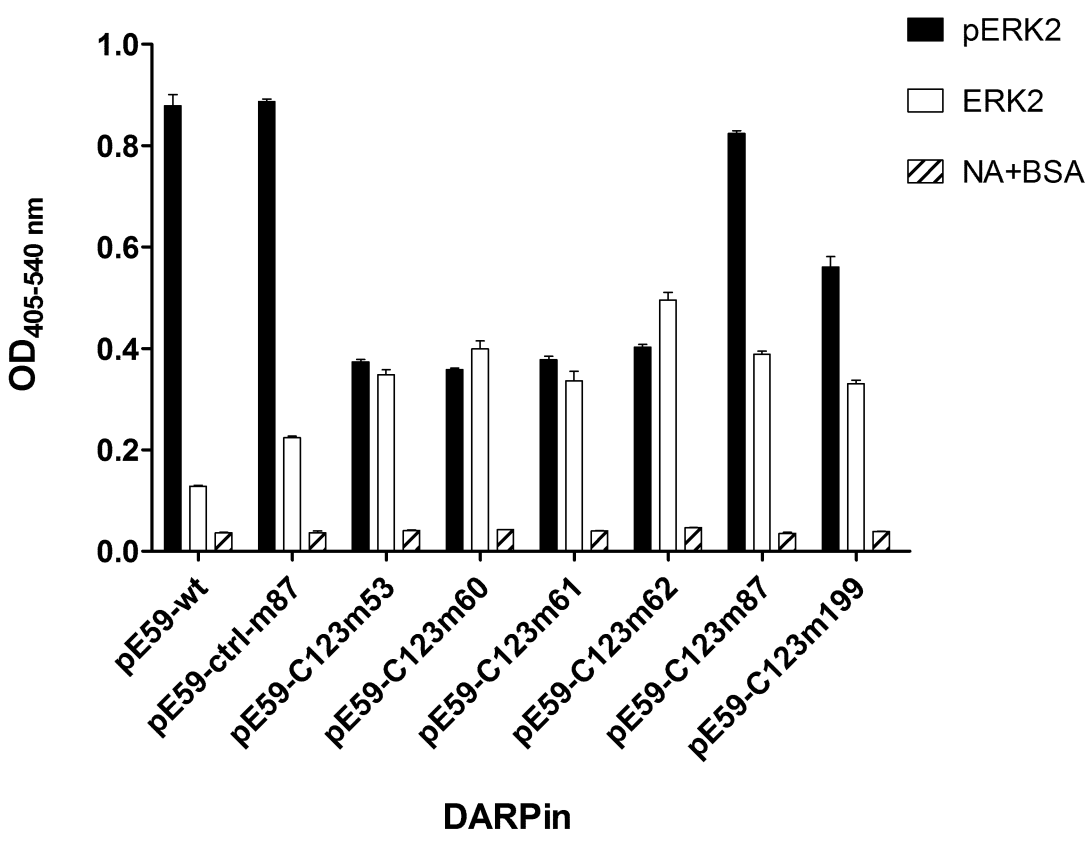

Supplemental Figure 4 | Binding specificity of DARPin pE59-C123m. DARPin/mero conjugates (pE59-C123m) derived from pE59 (pE59-wt) containing a cysteine at residue Asn123 were tested for ERK2 phosphorylation-specific interaction with ELISA. pE59-ctrl-m87 contains a mero87-labeled cysteine at the N-terminus of the DARPin, a region which is not implicated in binding to phosphorylated ERK2 (pERK2). In addition, binding to wells with neutravidin (NA) and bovine serum albumin (BSA) only was assessed. The absorption was measured at 405 nm with background wavelength correction at 540 nm ($OD_{405\text{-}504\ nm}$).

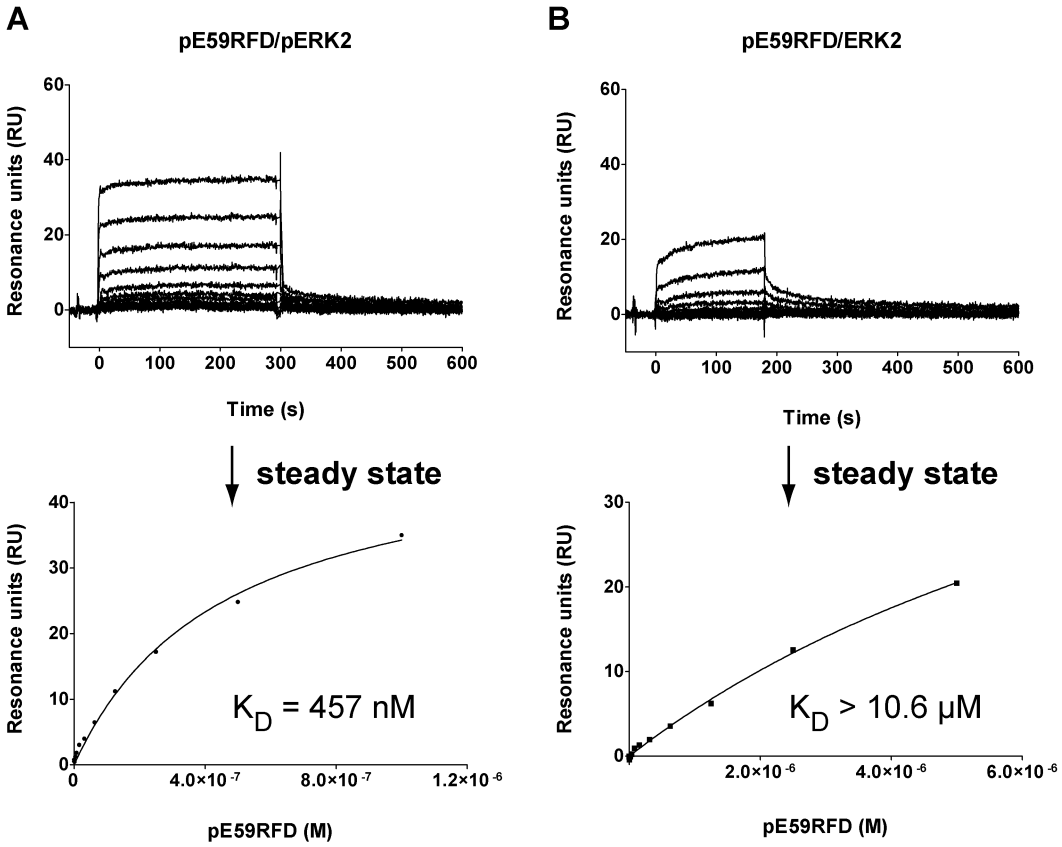

Supplemental Figure 5 | Affinity determination of DARPin sensor pE59RFD using SPR. The binding kinetics of mero-conjugated DARPin pE59RFD were analyzed using Biacore. The data were evaluated by fitting the equilibrium binding responses to obtain K_D values. (A) Binding of varied amounts of pE59RFD (0.24, 0.48, 0.9, 1.9, 3.9, 7.8, 15.6, 31.25, 62.5, 125, 250, 500 and 1000 nM) to pERK2 was monitored and compared to an empty flow cell. (B) Increasing concentrations of pE59RFD (0.6, 1.2, 2.4, 4.9, 9.8, 19.5, 39.1, 78.1, 156.3, 312.5, 625, 1250, 2500 and 5000 nM) were applied to immobilized ERK2 and compared to an empty flow cell.

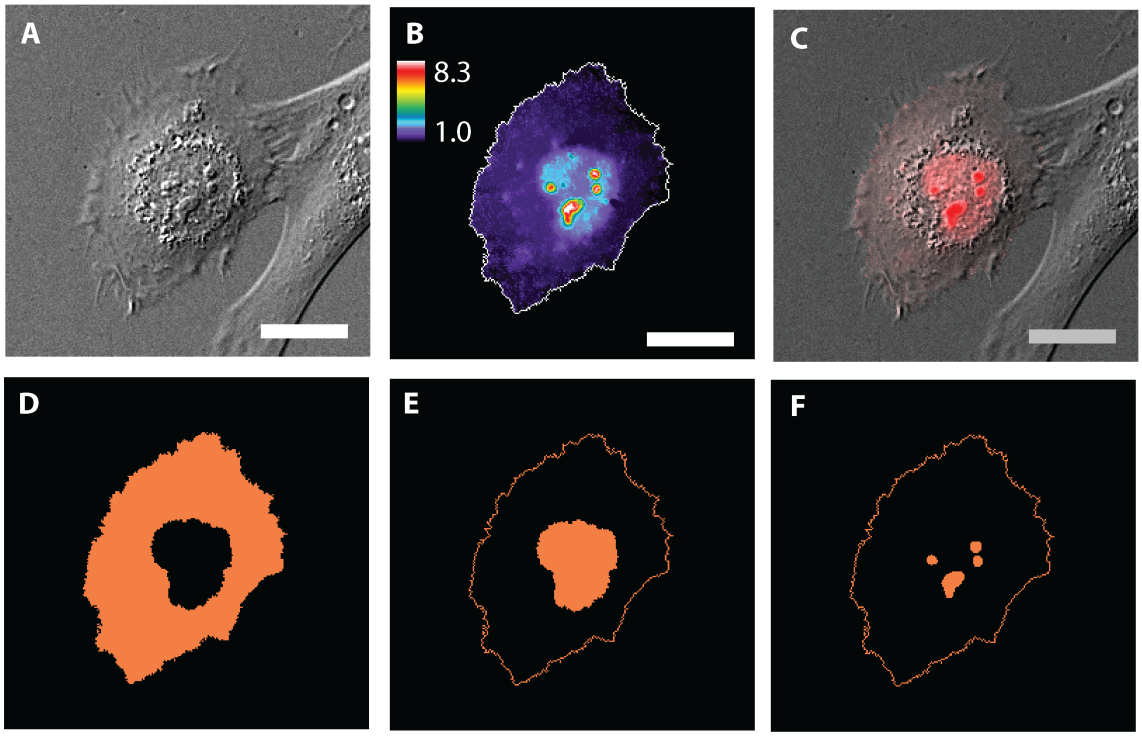

Supplemental Figure 6 | Quantification of ERK activity. Scale bar: 20 μm. (A) Differential interference contrast (DIC) image. (B) Ratio image. (C) Overlay of the DIC and ratio images. (D) Cytoplasmic mask for AvgRatioCytoplasm. (E) Nucleus mask for AvgRationucleus. (F) Nucleolus mask for AvgRationucleolus.

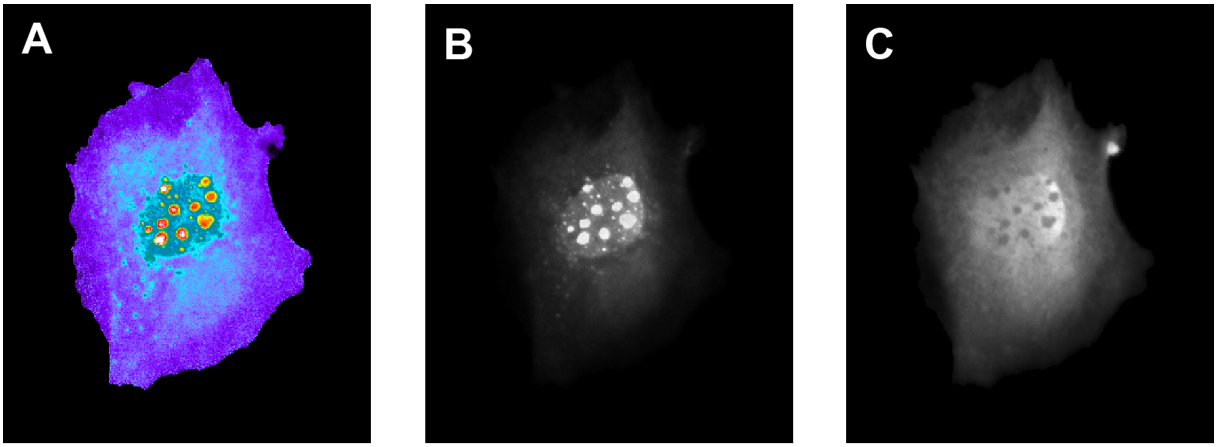

Supplemental Figure 7 | Demonstration of increased activity of ERK in the nucleolus by direct comparison of the dye channel and the YFP channel. ERK activity was quantified as the ratio of dye fluorescence intensity/YFP intensity. The single channels are also shown. The increase in dye fluorescence by far overcomes a very slight exclusion of YFP.

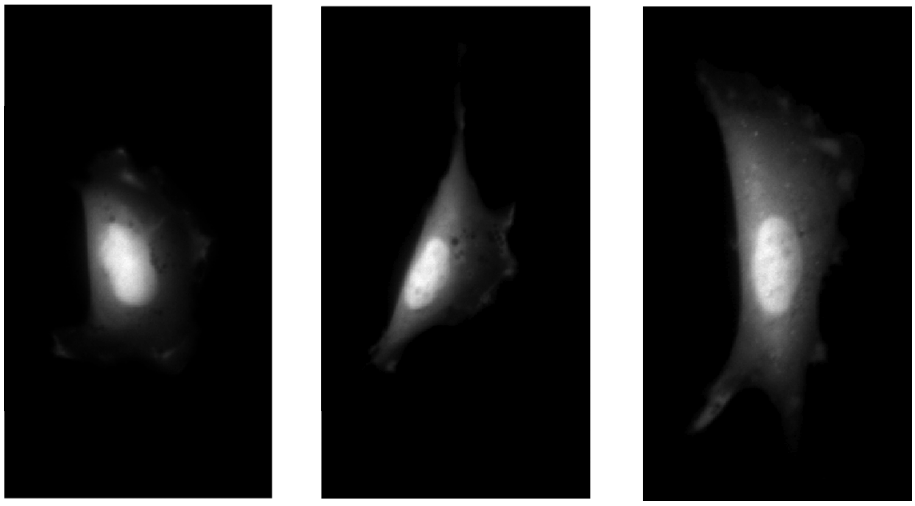

Supplemental Figure 8 | Control study: Absence of DARPin enrichment in the nucleolus shown by inhibition. Background fluorescence of the dye on the sensor was measured in the presence of the MEK1/2 inhibitor U0126. Typical cells are shown.

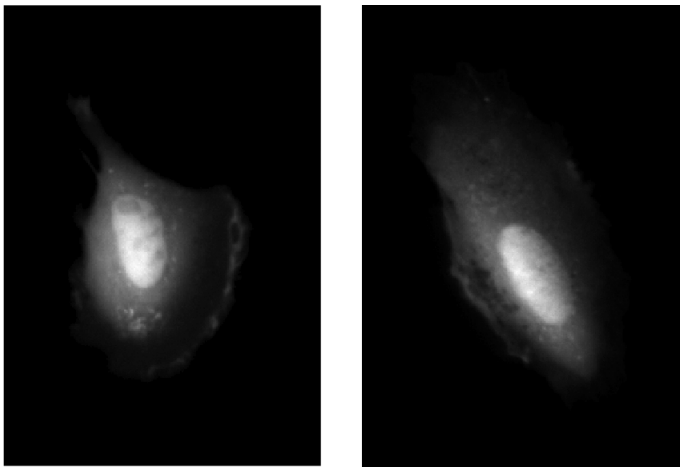

Supplemental Figure 9 | Control study: Absence of DARPin enrichment in the nucleolus shown by mutation. Background fluorescence of the dye on the mutated weak-binding sensor (DARPin-pE59 with D46A/R90A) was measured. Typical cells are shown.

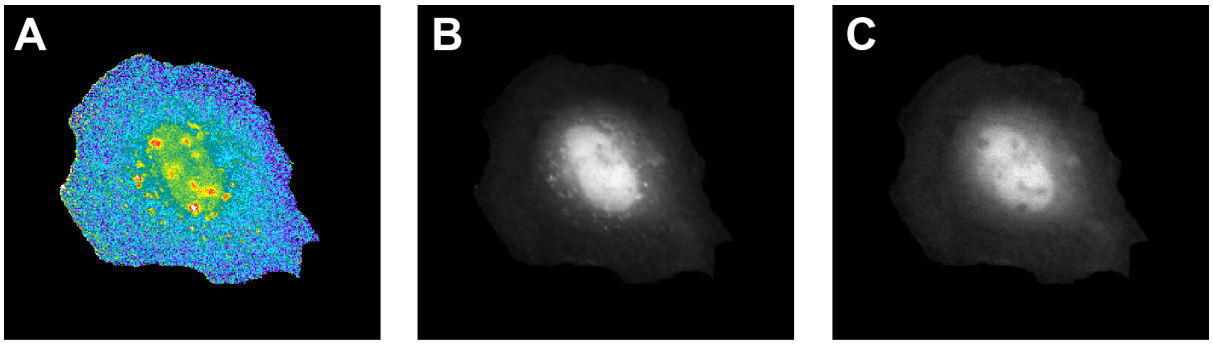

Supplemental Figure 10 | Control study: direct attachment of DARPin and mCerulean. A Gly-Ser-Gly-Ser-Gly-Ser-Gly-Ser-Gly-Ser-Gly-Ser-Gly-Ser-Gly-Ser linker was used to join the C-terminus of monomeric Cerulean fluorescent protein to the N-terminus of the DARPin N123 binder. ERK activity was quantified as the ratio of dye fluorescence intensity/mCerulean intensity. The single channels are also shown